



PEG-combined liquid phase synthesis and electrochemical properties of carbon-coated $\text{Li}_3\text{V}_2(\text{PO}_4)_3$

Ren-heng WANG, Xin-hai LI, Zhi-xing WANG, Hua-jun GUO, Bin HUANG

School of Metallurgy and Environment, Central South University, Changsha 410083, China

Received 27 May 2014; accepted 24 July 2014

Abstract: The carbon-coated monoclinic $\text{Li}_3\text{V}_2(\text{PO}_4)_3$ (LVP) cathode materials were successfully synthesized by liquid phase method using PEG as reducing agent and carbon source. The effects of relative molecular mass of PEG on the properties of $\text{Li}_3\text{V}_2(\text{PO}_4)_3/\text{C}$ were evaluated by X-ray diffraction (XRD), scanning electron microscope (SEM) and electrochemical performance tests. The SEM images show that smaller size particles are obtained by adding larger and smaller PEGs. The electrochemical cycling of $\text{Li}_3\text{V}_2(\text{PO}_4)_3/\text{C}$ prepared by both PEG200 and PEG20k has a high initial discharge capacity of 131.1 mA·h/g at 0.1C during 3.0–4.2 V, and delivers a reversible discharge capacity of 123.6 mA·h/g over 30 cycles, which is better than that of other samples. The improvement in electrochemical performance is caused by its improved lithium ion diffusion coefficient for the macroporous morphology, which is verified by cyclic voltammetry (CV) and electrochemical impedance spectroscopy (EIS).

Key words: lithium-ion battery; lithium vanadium phosphate; PEG; carbon-coating; liquid phase method

1 Introduction

Lithium-ion batteries are considered the most advanced electrical energy storage and transfer systems. Recently, framework materials based on the phosphate polyanion have been extensively investigated as positive materials for Li-ion battery. The lithiated transition metal phosphates based on either the olivine or NASICON structure, such as LiMPO_4 ($M=\text{Fe}, \text{Co}, \text{Ni}, \text{and Mn}$) [1–4], $\text{Li}_3\text{M}_2(\text{PO}_4)_3$ ($M=\text{Fe}$ and V) [5] and LiVPO_4F [6,7]. Contrasting to the commercial layered LiCoO_2 material utilized as the positive electrode suffering from high cost and inferior safety concerns [8–10], the olivine-phase LiFePO_4 and monoclinic $\text{Li}_3\text{V}_2(\text{PO}_4)_3$ (LVP) have attracted extensive interest among researchers due to their high theoretical capacity, acceptable operating voltage, good cycle life, low cost and superior safety [11].

Otherwise than the olivine-phase LiFePO_4 with only one lithium extraction/insertion site, the monoclinic LVP with three-dimensional (3D) framework contains three independent lithium sites, which can overcome the electronic and lithium diffusion limitations, improve the rate of extraction/insertion and hence the power

density of battery, and optimize the electrochemical performance under high-current regimes [12–14]. The large poly-anion instead of the smaller O^{2-} ions in an open 3D framework helps to stabilize the structure and allows fast ion migration [15,16].

However, the main drawbacks of pristine LVP are its very low intrinsic electronic conductivity which results in poor cycling stability and rate performance, which has lower electronic conductivity about 2.3×10^{-8} S/cm at 300 K because of the polarization of V—O bond [17]. This makes it difficult to utilize LVP cathode material fully in lithium ion batteries [18,19]. To solve the problem, there are three main ways, such as metal ion doping [20,21], particle size reducing [22], and carbon coating [11,23].

In order to overcome the poor conductivity, in this work, LVP/C cathode samples were first synthesized by liquid phase method using both PEG with high relative molecular mass and low relative molecular mass as carbon sources. As a surfactant and dispersing agent, PEG can effectively inhibit the aggregation of colloidal particles during the formation of the gel. Meanwhile, PEG will coat on the particles to play the role of carbon source during the sintering [24], and the resulting electrochemical lithium extraction/insertion properties

were investigated.

2 Experimental

The LVP cathode materials were prepared by liquid phase method using $\text{LiOH}\cdot\text{H}_2\text{O}$ (A.R.), V_2O_5 (A.R.), $(\text{NH}_4)_2\text{HPO}_4$ (A.R.), PEG20k (A.R.), and PEG200/400/600 (A.R.) as starting materials. Rheological phase reaction proceeding is shown in Fig. 1. The reactants had the same molar ratio ($\text{Li}:\text{V}:\text{P}:\text{PEG}=3:2:3:2$), and $\text{PEG20k}:\text{PEG200}/400/600 = 1:1$ in the mass ratio. The carbon-coated LVP/C composites were prepared by CTR method where the carbon source was used as the reducing agent instead of H_2 gas. The carbon can be obtained by the decomposition of PEG. Firstly, stoichiometric V_2O_5 powder was dissolved in a hydrogen peroxide solution (30%, mass fraction), then an exothermic reaction occurred, resulting in the partial decomposition of hydrogen peroxide. And then a red brown solution was obtained. Secondly, stoichiometric $\text{LiOH}\cdot\text{H}_2\text{O}$, $(\text{NH}_4)_2\text{HPO}_4$ and PEG20k, were added to the above $\text{V}_2\text{O}_5\cdot n\text{H}_2\text{O}$. The mixture was vibrated in the ultrasonic oscillator for 5 min. And then PEG200/400/600 was added to the above mixture. Finally, the mixture was evaporated at $50\text{ }^\circ\text{C}$ for 0.5–1 h with a rotary evaporator until it was dried. Then the mixture was dried at $80\text{ }^\circ\text{C}$ in the oven. The precursors were then ground and burned at $800\text{ }^\circ\text{C}$ for 15 h with flowing argon gas to yield the LVP/C composite materials.

The phase identification of the LVP compounds was carried out by X-ray diffraction (XRD; Rint-2000, Rigaku) using $\text{Cu K}\alpha$ radiation in the 2θ range from 10° to 60° . The morphologies of the powders were observed by scanning electron microscope (SEM; JEOL, JSM-5600LV). The carbon contents of samples were

determined by a carbon–sulfur analyzer (Multi EA2000).

The electrochemical measurements were performed using CR2025 coin-type cells. The cathodes of the two-electrode electrochemical cells were fabricated by blending the prepared powder with acetylene black and polyvinylidene fluoride (PVDF) binder in a mass ratio of 8:1:1 in *N*-methyle-2-pyrrolidone (NMP). The slurry cathode mixture was pasted on an Al foil and dried at $80\text{ }^\circ\text{C}$ for 24 h in vacuum oven. The electrolyte was 1 mol/L lithium hexafluorophosphate (LiPF_6) solution dissolved in ethylene carbonate (EC) and dimethyl carbonate (DMC) (volume ratio of 1:1). The separator was Celgard 2300. CR2025 coin cells were assembled in an argon-filled dry glove box, and then the cells were measured using Land CT2001A (Wuhan, China) battery tester. The electrochemical measurements were performed at 0.1C rate in a voltage range of 3.0–4.2 V versus Li/Li^+ at room temperature.

The cyclic voltammetry (CV) test was carried out on a CHI 860D electrochemical workstation (GL10AD, Beijing, China) with a three-electrode system incorporating LiMn_2O_4 as the working electrode and Li foils as counter and reference electrodes at a scanning rate of 0.1 mV/s between 3.0 and 4.2 V. Electrochemical impedance spectrum (EIS) experiments were carried out with the frequency range from 10 kHz to 10 mHz with an alternating current (AC) voltage of 5 mV.

3 Results and discussion

3.1 XRD analysis

The X-ray diffraction patterns of the prepared LVP/C composites are shown in Fig. 2. The amounts of carbons in the LVP/C composite with PEG20k+200, PEG20k+400 and PEG20k+600 are respectively about 10.21%, 8.53% and 14.94%, determined by C–S

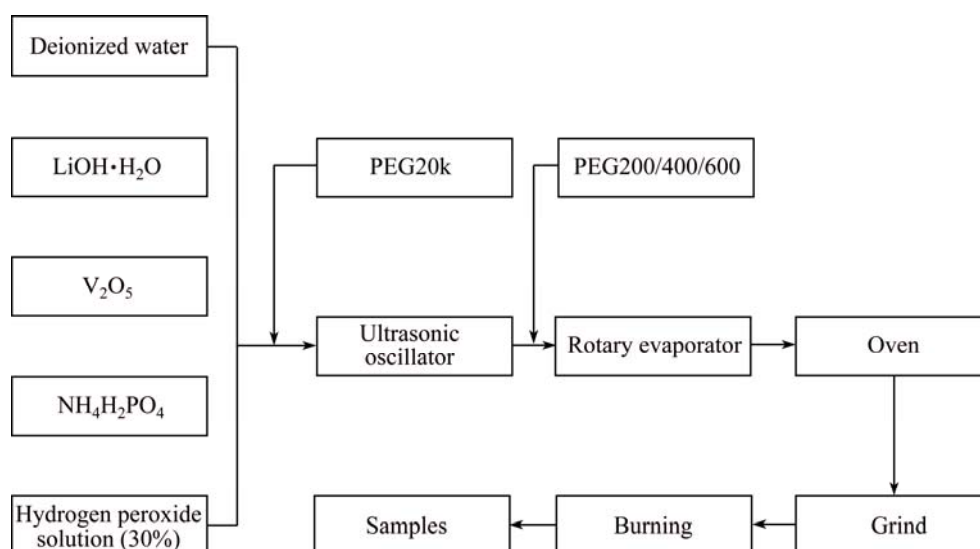


Fig. 1 Synthetic route of LVP/C with different combined PEG

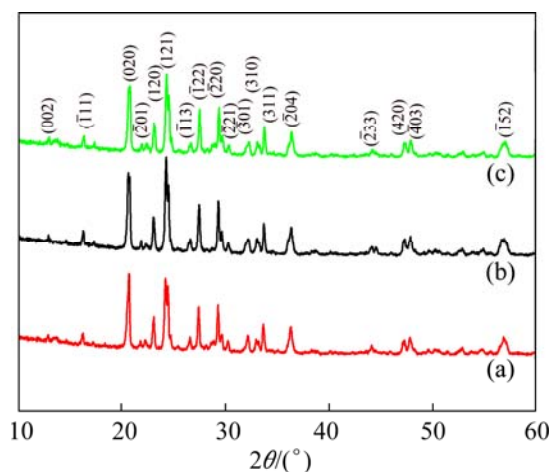


Fig. 2 XRD patterns of LVP/C composites synthesized with PEG20k+200 (a), PEG20k+400 (b) and PEG20k+600 (c)

analysis method [24]. The patterns of all samples are similar to each other. No evidence of diffraction peaks for crystalline carbon (graphite) appeared in the diffraction pattern. It can be seen that the experiments with all samples have produced a single phase of LVP with monoclinic structure, which means that the PEG would not alter the structure of materials. The high chemical activity of carbon ensures carbon on the surface of freshly formed LVP/C particles by the in situ coating. All the diffraction peaks can be indexed monoclinic structure of space group $P2_{1/n}$ [25], which is consistent with the previous reports [26,27]. The observed and calculated patterns match very well.

3.2 SEM analysis

Although monoclinic LVP has been stated as a high rate cathode, in the previous studies, it had been reported that the morphology and surface area of obtained particles still have the notable influence on the cycle performance [28]. The morphology of the obtained LVP/C materials was observed by SEM as shown in Fig. 3. The particles prepared with PEG20k+200 were smaller than those prepared with PEG20k+400 and PEG20k+600. When the relative molecular mass was PEG20k+200, the particles agglomerated, it was advantageous to increase the tap density of cathode materials. The particles congregated together with an average size of 1 μm . This indicated that the small relative molecular mass inhibited the particle growth during a sintering process. In addition, for the samples, their surface was rough, and some small particles bounded on the surface of LVP/C were observed, which can be considered as small scattered carbon particles. In those particles with a large diameter and a relative large specific area, the Li ions have diffusion over great distance between the surface and center during lithium

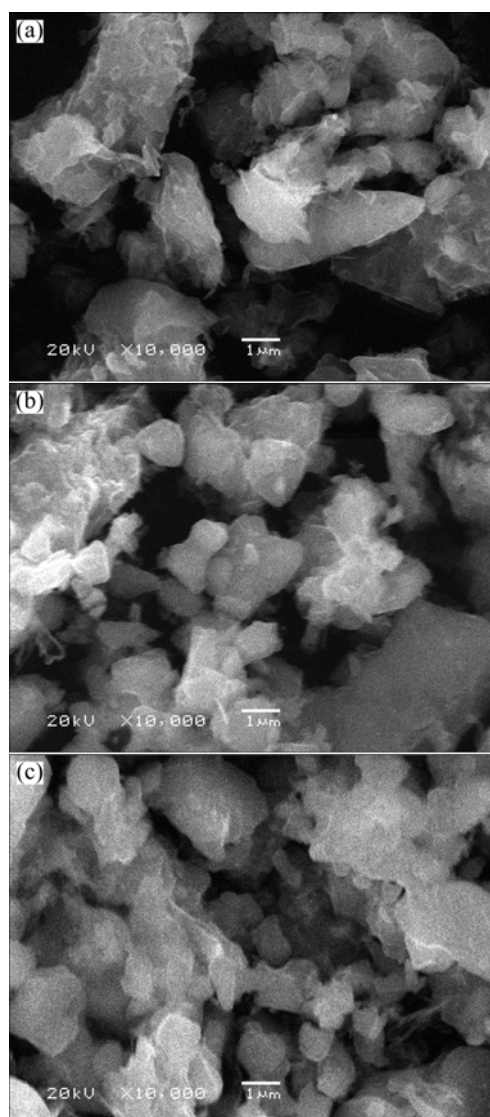


Fig. 3 SEM images of LVP/C composites synthesized with PEG20k+600 (a), PEG20k+400 (b), and PEG20k+200 (c)

insertion or extraction, and the active material near the center of particle contributes very large to the charge/discharge reaction [19].

3.3 Cycling performance of cells

The initial charge–discharge performances at 0.1C rate were measured at room temperature between 3.0–4.2 V. As shown in Fig. 4, there are three voltage plateaus around 3.59, 3.68 and 4.08 V in the charge process, and corresponding three discharge plateaus around 3.57, 3.65 and 4.05 V, which are identified as the two-phase transition process during the electrochemical reaction. In charge process, the first lithium ion is extracted in two steps, 3.6 and 3.7 V, because of the presence of an ordered phase $\text{Li}_{2.5}\text{V}_2(\text{PO}_4)_3$. Subsequently, the second lithium ion is extracted in one single plateau of 4.1 V to form $\text{Li}_{1.0}\text{V}_2(\text{PO}_4)_3$ [29]. These initial three plateaus are related to the two lithium ions extraction

which is associated with the V^{3+}/V^{4+} redox couple. The initial specific charge capacities of PEG20k+200, PEG20k+400, and PEG20k+600 are about 137.7, 137.3 and 131.3 mA·h/g, respectively. The initial specific discharge capacities of PEG20k+200, PEG20k+400, and PEG20k+600 are separately 131.1, 127.4 and 122.0 mA·h/g. As shown in Table 1, it is clear that the Coulombic efficiencies of the initial charge–discharge cycle are about 95.2% (PEG20k+200), 92.8% (PEG20k+400), and 92.9% (PEG20k+600). The result of the discharge capacity of the PEG20k+200 (131.1 mA·h/g) is very close to its practically available capacity (132 mA·h/g). Apparently, the initial discharge capacity of PEG20k+200 is better than others, which should be attributed to the effect of macroporous morphology. The small voltage polarization also suggests that the LVP/C electrode should have high electrochemical reversibility. From above all, the results show that using both much lower relative molecular mass and higher relative molecular mass can control the morphology and size of the particles.

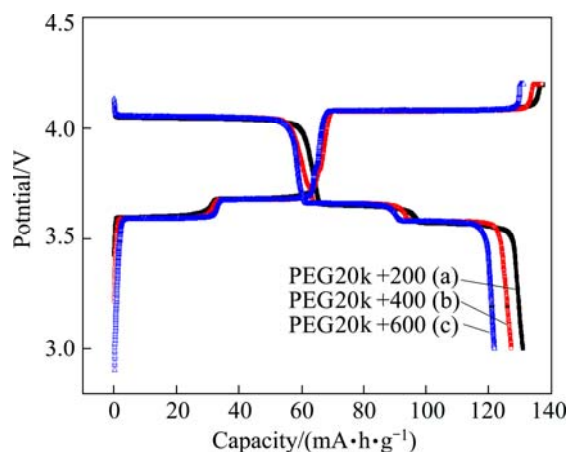


Fig. 4 Initial charge–discharge curves of LVP/C samples at 0.1C rate between 3.0 and 4.2 V

Table 1 Electrochemical performances of LVP/C with different combined PEG in initial charge–discharge at 0.1C

Sample	Capacity/(mA·h·g ⁻¹)		Coulombic efficiency/%
	Charge	Discharge	
PEG20k+200	137.7	131.1	95.2
PEG20k+400	137.3	127.4	92.8
PEG20k+600	131.3	122.0	92.9

The cycle performances of the prepared LVP/C samples evaluated in the Li/LVP cell configuration in the range of 3.0–4.2 V at room temperature are shown in Fig. 5. The voltage cut-offs were chosen according to Ref. [30]. As shown in Fig. 5 and Table 2. The capacity loss of PEG20k+200 is about 5.7% at 0.1C, 4.3% at 0.5C and 0.2% at 1C after 30 cycles. For PEG20k+400, after

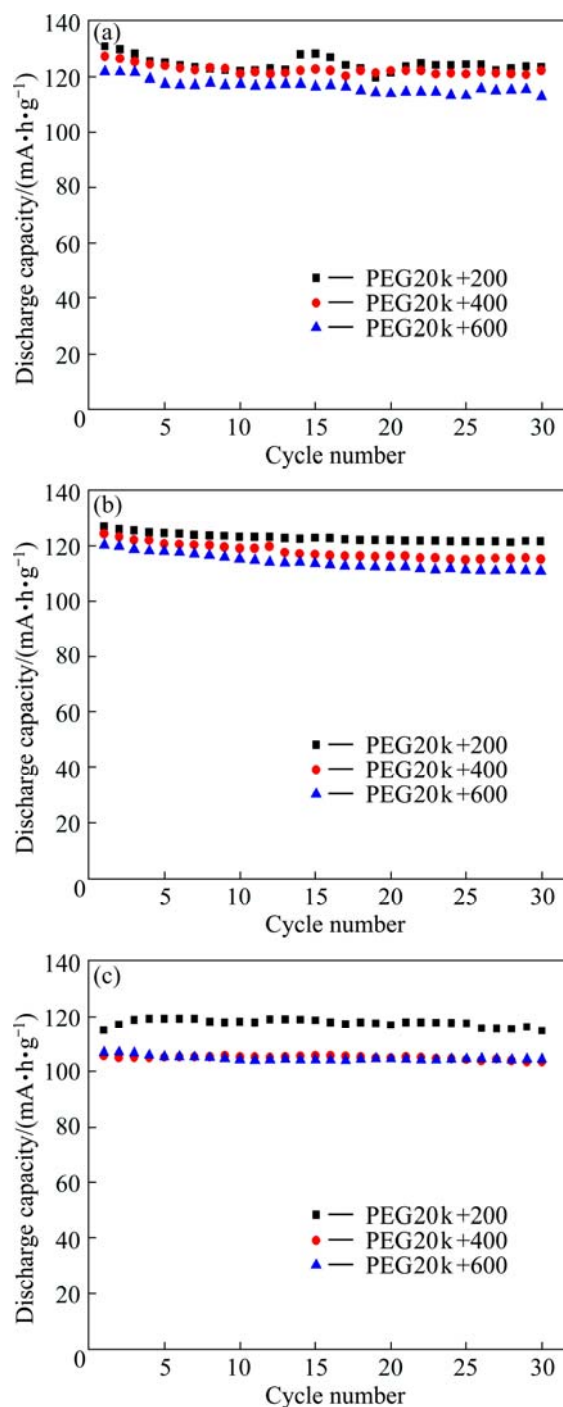


Fig. 5 Electrochemical cycling performances of PEG20k+200, PEG20k+400, and PEG20k+600 at 0.1C (a), 0.5C (b) and 1C (c) rate between 3.0 and 4.2 V

Table 2 Electrochemical performances of LVP/C with different combined PEGs after 30 cycles

Sample	Capacity/(mA·h·g ⁻¹)		
	0.1C	0.5C	1C
PEG20k+200	123.6	121.7	115
PEG20k+400	122.4	115.2	103.7
PEG20k+600	113.2	111	104.6

30 cycles, the capacity loss is about 3.9% at 0.1C, 7.5% at 0.5C and 2.0% at 1C. And the capacity loss of PEG20k+600 is about 7.2% at 0.1C, 7.9% at 0.5C and 2.3% at 1C after 30 cycles. It can be concluded that the LVP/C synthesized with relative molecular mass PEG20k+200 by liquid phase possesses better cycling performance than others. The good cycle life and excellent rate capability of the electrode may be attributed to the relative invariance of monoclinic LVP host framework and highly uniform distribution of carbon in the LVP particles.

3.4 Impedance analysis

To clarify the improvement of cyclic stability of LVP/C with PEG20k+200, electrochemical kinetic property of LVP/C was investigated by electrochemical impedance spectroscopy (EIS). The lithium ion diffusion coefficient was calculated from the following formulas [31]:

$$D = R^2 T^2 / 2 A^2 n^4 F^4 c \sigma^2 \quad (1)$$

$$Z_{re} = R_D + R_L + \sigma \omega^{1/2} \quad (2)$$

where R is the mole gas constant, T is the thermodynamic temperature, A is the surface area of the cathode, n is the number of electrons per molecule during oxidization, F is the Faraday constant, c is the concentration of lithium ion, σ is the Warburg factor that is relative with Z_{re} .

As shown in Fig. 6, there are three regions, two semicircles and an inclined line. The semicircle at high-frequency region is attributed to the charge transfer resistance (R_{ct}), and the straight line at lower frequency corresponds to Li^+ diffusion resistance in electrode bulk, namely the Warburg impedance. The numerical value of diameter of the semicircle on the real axis is approximate equal to R_{ct} . From Fig. 6, it is clear that the charge-transfer impedance for PEG20k+200 sample is

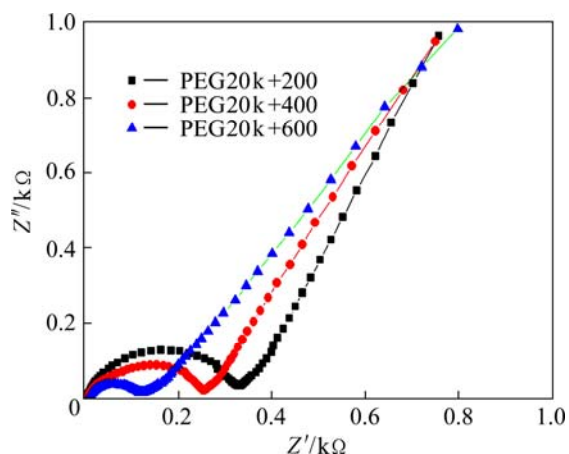


Fig. 6 Impedance spectra of PEG20k+200, PEG20k+400, and PEG20k+600 at discharge potential of 3.0 V during the second cycle

much lower than those for the other two samples, indicating that the combination of different relative molecular masses may increase the electronic conductivity and improve the Li^+ diffusion, which is well consistent with its good rate performance measured as above. This result is similar to those in the previous reports [23]. It is due to the decrease of grain size and improved homogeneity of the carbon dispersion.

3.5 CV measurements

Figure 7 demonstrates the initial cyclic voltammetry (CV) curves for three samples at the scanning rate of 0.05 mV/s in a voltage range of 3.0–4.5 V (vs Li/Li^+). Three curves of the electrodes showed a similar profile, which indicated that the reaction mechanism was not changed during the lithium extraction/insertion process, while all redox peaks were shifted. There are three pairs of redox peaks with the oxidation peaks located at around 3.66, 3.75 and 4.166 V, coupling with three reduction peaks at about 3.51, 3.59 and 3.97 V, respectively, which are in good agreement with charge–discharge curves as shown in Fig. 5. The oxidation peaks located around 3.65 and 3.75 V correspond to the removal of the first Li in two steps, because there is an ordered $\text{Li}_{2.5}\text{V}_2(\text{PO}_4)_3$ phase. It should also be noted that the lithium extraction and insertion processes for the PEG20k+200 sample are much more ordered than that of PEG20k+400 sample or PEG20k+600 sample, as evidenced by the emergence of relatively more intense and sharper peaks. The relative narrow gap of redox peaks and more ordered Li^+ extraction/insertion processes indicate that the PEG20k+200 sample has smaller voltage polarization and better electrochemical reversibility than those of others. This keeps well with the results that the specific capacity of LVP with PEG20k+200 measured at 0.1C rate is higher than those of others.

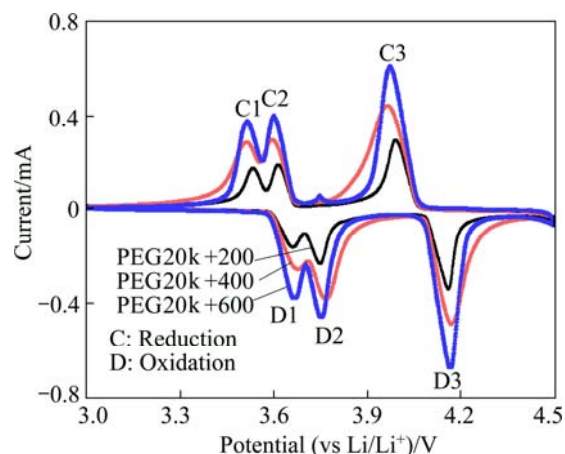


Fig. 7 Cyclic voltammetry (CV) curves of PEG20k+200, PEG20k+400 and PEG20k+600 at scanning rate of 0.005 mV/s in second cycle

4 Conclusions

1) XRD results show that no other impurity is detected. The LVP/C composite with an average size of about 1 μm presents large reversible capacity, good rate capability, and excellent cyclic stability in the region of 3.0–4.2 V.

2) Compared with others, PEG20k+200 sample shows better reversible capacity and improves rate capability. The initial discharge capacities of PEG20k+200 sample are 131.1, 127.2, and 115.2 mA·h/g at 0.1C, 0.5C and 1C, respectively. After 30 cycles, the cells deliver the discharge capacity of 123.6, 121.7 and 115 mA·h/g at 0.1C, 0.5C and 1C and retain 92.8%, 95.7% and 99.8% of its initial discharge capacity.

3) One of the reasons may be beneficial to the extrinsic properties. In those particles with a large diameter and a relatively low specific area, the Li ions diffuse over great distance between the surface and center during lithium insertion or extraction, and the active material near the center of particle contributes very large to the charge–discharge reaction.

References

- [1] LIU P, WANG J, HICKS-GARNER U, SHERMAN E, SOUKIAZIAN S, VERBRUGGE M, TATARIA H, MUSSER J, FINAMORE P. Aging mechanisms of LiFePO₄ batteries deduced by electrochemical and structural analyses [J]. *Journal of the Electrochemical Society A*, 2010, 157: 499–507.
- [2] TANG Hao, TAN Long, XU Jun. Synthesis and characterization of LiFePO₄ coating with aluminum doped zinc oxide [J]. *Transaction of Nonferrous Metals Society of China*, 2013, 23: 451–455.
- [3] VINODKUMAR E, ROTEM M, RAN E, GREGORY S, DORON A. Challenges in the development of advanced Li-ion batteries: A review [J]. *Energy Environ Sci*, 2011, 4: 3243–3262.
- [4] LI H H, JIN J, WEI J P, ZHOU Z, YAN J. Fast synthesis of core-shell LiCoPO₄/C nanocomposite via microwave heating and its electrochemical Li intercalation performances [J]. *Electrochem Commun*, 2009, 11: 95–98.
- [5] DING Yan-huai, ZHANG Ping. Effect of Mg and Co co-doping on electrochemical properties of LiFePO₄ [J]. *Transaction of Nonferrous Metals Society of China*, 2012, 22(S1): s153–s156.
- [6] ZHONG Sheng-kui, CHEN Wen, LI Yan-hong, ZOU Zheng-guang, LIU Chang-jiu. Synthesis of LiVPO₄F with high electrochemical performance by sol-gel route [J]. *Transaction of Nonferrous Metals Society of China*, 2010, 20(S1): s275–s278.
- [7] REDDY M V, RAO G V S, CHOWDARI B V R. Long-term cycling studies on 4V-cathode, lithium vanadium fluorophosphates [J]. *J Power Sources*, 2010, 195: 5768–5774.
- [8] SCROSATI B. Challenge of portable power [J]. *Nature*, 1995, 373: 557–558.
- [9] WHITTINGHAM M S. Lithium batteries and cathode materials [J]. *Chem Rev*, 2004, 104: 4271–4302.
- [10] GREY C P, DUPRE N. NMR studies of cathode materials for lithium-ion rechargeable batteries [J]. *Chem Rev*, 2004, 104: 4493–4512.
- [11] SU J, WU X L, LEE J S, KIMB J K, GUO Y G. A carbon-coated Li₃V₂(PO₄)₃ cathode material with an enhanced high-rate capability and long lifespan for lithium-ion batteries [J]. *J Mater Chem A*, 2013, 1: 2508–2514.
- [12] NANJUNDASWAMY K S, PADHI A K, GOODENOUGH J B, OKADA S, OHTSUKA H, ARAI H, YAMAKI J. Synthesis, redox potential evaluation and electrochemical characteristics of NASICON-related-3D framework compounds [J]. *Solid State Ionics*, 1996, 92: 1–2.
- [13] GAUBICHER J, WURM C, GOWARD G, MASQUELIER C, NAZAR L. Rhombohedral form of Li₃V₂(PO₄)₃ as a cathode in Li-ion batteries [J]. *Chem Mater*, 2000, 12: 3240–3242.
- [14] HUANG H, YIN S C, KERR T, TAYLOR N, NAZAR L F. Nanostructured composites: A high capacity, fast rate Li₃V₂(PO₄)₃/carbon cathode for rechargeable lithium batteries [J]. *Adv Mater*, 2002, 14: 1525–1528.
- [15] RUI X H, SIM D H, WONG K G, ZHU J X, LIU W L, XU C, TAN H T, XIAO N, HNG H H, LIM T M, YAN Q Y. Li₃V₂(PO₄)₃ nanocrystals embedded in a nanoporous carbon matrix supported on reduced graphene oxide sheets: Binder-free and high rate cathode material for lithium-ion batteries [J]. *J Power Sources*, 2012, 214: 171–177.
- [16] SAIDI Y, BARKER J, HUANG H, SOWYER J L, ADAMSON G. Electrochemical properties of lithium vanadium phosphate as a cathode material for lithium-ion batteries [J]. *Electrochem Solid State Lett A*, 2002, 12: 149–151.
- [17] YIN S C, GRONDER H, STROBEL P, ANNE M, NAZAR L F. High performance biodegradable materials [J]. *Chem Mater*, 2003, 16: 1456–1465.
- [18] ZHONG S K, YIN Z L, WANG Z X, GUO H J, LI X H. Synthesis and characterization of novel cathode material Li₃V₂(PO₄)₃ by carbon-thermal reduction method [J]. *Transaction of Nonferrous Metals Society of China*, 2006, 16(S): s708–s710.
- [19] SAIDI Y, BARKER J, HUANG H, SOWYER J L, ADAMSON G. Performance characteristics of lithium vanadium phosphate as a cathode material for lithium-ion batteries [J]. *J Power Sources*, 2003, 119–121: 266–272.
- [20] ZHANG B, LIU J Q, ZHANG Q, LI Y H. Electrochemical performance of Al-substituted Li₃V₂(PO₄)₃ cathode materials synthesized by sol-gel method [J]. *Transaction of Nonferrous Metals Society of China*, 2010, 20: 619–623.
- [21] WANG R H, XIAO S H, LI X H, WANG J X, GUO H J, ZHONG F X. Structural and electrochemical performance of Na-doped Li₃V₂(PO₄)₃/C cathode materials for lithium-ion batteries via rheological phase reaction [J]. *J Alloys Compd*, 2013, 575: 268–272.
- [22] DELACOURT C, POIZOT P, LEVASSEUR S, MASQUELIER C. Size effects on carbon-free LiFePO₄ powders [J]. *Electrochem Solid State Lett*, 2006, 9: 352–355.
- [23] CHANG C X, XING J F, SHI X X, HAN X X, YUAN L J, SUN J T. Rheological phase reaction synthesis and electrochemical performance of Li₃V₂(PO₄)₃/carbon cathode for lithium ion batteries [J]. *Electrochim Acta*, 2008, 53: 2232–2237.
- [24] ZHONG S K, CHEN W, WU L, LIU J Q. A PEG-assisted rheological phase reaction synthesis of 5LiFePO₄·Li₃V₂(PO₄)₃/C as cathode material for lithium ion cells [J]. *Ionics*, 2012, 18: 523–527.
- [25] MORGAN D, CEDER G, SAIDI M Y. Experimental and computational study of the structure and electrochemical properties of Li_xM₂(PO₄)₃ compounds with the monoclinic and rhombohedral structure [J]. *Chem Mater*, 2002, 14: 4648–4693.
- [26] WANG L J, ZHOU X C, GUO Y L. Synthesis and performance of carbon-coated Li₃V₂(PO₄)₃ cathode materials by a low temperature solid-state reaction [J]. *J Power Sources*, 2010, 195: 2844–2850.
- [27] QIAO Y Q, TU J P, XIANG J Y, WANG X L, MAI Y J, ZHANG D, LIU W L. Effects of synthetic route on structure and electrochemical performance of Li₃V₂(PO₄)₃/C cathode materials [J]. *Electrochimica*

- Acta, 2011, 56: 4139–4145.
- [28] QIAO Y Q, TU J P, WANG X L, GU C D. The low and high temperature electrochemical performances of $\text{Li}_3\text{V}_2(\text{PO}_4)_3/\text{C}$ cathode material for Li-ion batteries [J]. *J Power Sources*, 2012, 199: 287–292.
- [29] YIN S C, GRONGDER H, STROBEL P, ANNE M, NAZAR L F. Electrochemical property: Structure relationships in monoclinic $\text{Li}_{3-y}\text{V}_2(\text{PO}_4)_3$ [J]. *J Am Chem Soc*, 2003, 125: 10402–10411.
- [30] ZHONG S K, WANG J, LIU L T. Investigations on the synthesis and electrochemical performance of $\text{Li}_3\text{V}_2(\text{PO}_4)_3/\text{C}$ by different methods [J]. *Ionics*, 2010, 16: 117–121.
- [31] LIU J, CAO Q, FU L J, LI C, WU Y P, WU H Q. Doping effects of zinc on LiFePO_4 cathode material for lithium ion batteries [J]. *Electrochemistry Communication*, 2006, 8: 1553–1557.

液相法合成 PEG 组合包覆 $\text{Li}_3\text{V}_2(\text{PO}_4)_3$ 的电化学性能

王任衡, 李新海, 王志兴, 郭华军, 黄斌

中南大学 冶金与环境学院, 长沙 410083

摘要: 以聚乙二醇(PEG)作为还原剂和碳源, 采用流变法成功合成碳包覆的单斜晶系磷酸钒锂正极材料, 采用 XRD、SEM 和电化学性能测试手段考察不同相对分子质量组合的聚乙二醇对合成材料的影响。SEM 观察显示, 大相对分子质量和小相对分子质量的聚乙二醇组合有利于合成更小、更均匀的颗粒。相对分子质量为 200 和 20k 组合的聚乙二醇合成的磷酸钒锂在 0.1C, 3.0~4.2 V 电压范围进行充放电循环, 其首次放电比容量为 131.1 mA·h/g, 30 次循环后仍有 123.6 mA·h/g, 优于其他相对分子质量组合形式。通过 CV 和 EIS 图谱分析, 相对分子质量相差越大, 越有利于提高锂离子扩散系数, 从而改善材料的电化学性能。

关键词: 锂离子电池; $\text{Li}_3\text{V}_2(\text{PO}_4)_3$; 聚乙二醇(PEG); 碳包覆; 液相法

(Edited by Xiang-qun LI)